Proceedings of the ASME 2013 International Mechanical Engineering Congress and Exposition
IMECE2013
November 15-21, 2013, San Diego, California, USA

IMECE2013-65490

Experimental Characterization of Adsorption and Transport Properties for Advanced Thermo-Adsorptive Batteries

Hyunho Kim
Department of Mechanical Engineering
Massachusetts Institute of Technology
Cambridge, MA, USA

Sungwoo Yang
Department of Mechanical Engineering
Massachusetts Institute of Technology
Cambridge, MA, USA

Shankar Narayanan
Department of Mechanical Engineering
Massachusetts Institute of Technology
Cambridge, MA, USA

Ian McKay
Department of Mechanical Engineering
Massachusetts Institute of Technology
Cambridge, MA, USA

Evelyn N. Wang
Department of Mechanical Engineering
Massachusetts Institute of Technology
Cambridge, MA, USA

ABSTRACT

Thermal energy storage has received significant interest for delivering both heating and cooling in electric vehicles, to minimize the use of the on-board electric batteries for heating, ventilation and air-conditioning (HVAC). An advanced thermo-adsorptive battery (ATB) is currently being developed, to provide both heating and cooling for an electric vehicle. We present a detailed thermophysical and physicochemical characterization of adsorptive materials for the development of the ATB. We discuss the feasibility of using contemporary adsorptive materials, such as zeolite 13X, by carrying out a detailed experimental characterization. In this study, zeolite 13X is combined with aluminum hydroxide ($Al(OH)_3$) as a binder to improve the thermal conductivity. We also investigate the effect of densification on the overall transport characteristics of the adsorbent-binder composite material. Accordingly, the effective thermal conductivity, surface area, adsorption capacity and surface chemistry were characterized using the laser flash technique, surface sorption analyzer, thermogravimetric analyzer, and x-ray scattering technique. Thermal conductivity predictions of both zeolite 13X and its combination with the binder were made with existing conductivity models. Thermal conductivity in excess of 0.4 W/mK was achieved with the addition of 6.4 wt.% of $Al(OH)_3$. However, a 10.6 % decrease in adsorption capacity was also observed. The experimental characterization presented herein is an essential step towards the development of the proposed ATB for next-generation electric vehicles.

INTRODUCTION

Conventional HVAC system can significantly drain the electric battery in current EVs, which can adversely affect its drivable range [1]. This is a prominent disadvantage of current EVs compared to the conventional gasoline powered vehicles. Research over the past few decades on adsorption-based cooling and heating systems has revealed a significant potential for adsorption-based portable HVAC systems. High surface area zeolites [2, 3] and more recently, metal-organic frameworks (MOFs) [4-6] promise a technology replacement of current HVAC systems with high energy density adsorption-based systems. We are developing a compact and light-weight advanced thermo-adsorptive battery (ATB) for electric vehicles, which can provide both cooling and heating, support fast charging with negligible self-discharge rate. In order to achieve these goals, the ATB utilizes water as the refrigerant and adsorbents with high adsorption capacities even at low operating pressures. However, poor thermal transport characteristics can severely limit the adsorption capacities of such adsorbents. Therefore, effective heat dissipation during vapor adsorption is critical for maximizing the ATB performance. It is well known that the average thermal conductivity of conventional adsorbents is relatively small, matching those of typical ceramics and insulators. Due to their large micro-pore volume, adsorbents such as zeolites and MOFs, have low thermal conductivities [7, 8]. Consequently, these materials demonstrate poor thermal transport characteristics. In order to address this limitation, we are currently developing composite materials capable of providing

large adsorption capacities as well as higher thermal conductivities.

Aluminum hydroxide is known to increase effective thermal conductivity of zeolite composite without sacrificing the overall adsorption capacity at operational pressures corresponding to 60% relative humidity [9]. Consequently, in this study, zeolite 13X (NaX, Sigma Aldrich) and its combination with aluminum hydroxide were characterized by porosity analysis, thermogravimetric analyzers (TGA), surface sorption analyzer, X-ray diffraction (XRD), and laser flash technique for the measurement of thermal conductivity. We present our findings in the following sections.

NOMENCLATURE

α	Thermal Diffusivity
C_p	Specific Heat
D_p	Crystal Diameter
ΔP	Pressure Drop
ε	Porosity
k	Thermal Conductivity
L	Length
μ	Viscosity
Φ	Sphericity
ρ	Density
V	Flow Velocity
v	Volume Fraction

POROSITY ANALYSIS

Experimental characterization of porosity and its effect on the overall heat and mass transport phenomena using the adsorbent is an important step towards optimization of the ATB. The experiments used to determine porosity were also used to confirm the reported crystal density of zeolite 13X [10] (1470 kg/m^3), using the following relation between porosity and crystal density, shown in Equation (1):

$$\rho_{bulk} = \rho_{crystal}*(1-\varepsilon) \quad (1)$$

where, ρ_{bulk} denotes the density of bulk sample and $\rho_{crystal}$ is the crystal density of the sample.

A simple experimental set-up, shown in Figure 1, composed of a high pressure gas tank connected to a flow meter and a pressure transducer was used to measure the porosity and the crystal density of a sample fabricated by packing the adsorbent into a cylinder. Kozeny-Carman relation [11] for porous media, shown in Equation (2), was used for the calculation of porosity as a function of the adsorbent density, as shown in Figure 2:

$$\frac{\Delta P}{L} = \frac{180*V*\mu}{\varphi^2*D_p^2}\frac{(1-\varepsilon)^2}{\varepsilon^3} \quad (2)$$

In Equation (2), ΔP is the pressure drop across the packed sample, L is the length of the packed sample, V is the flow velocity, μ is the gas viscosity, ε is the porosity of the sample, φ is the sphericity of the sample, and D_p is the particle diameter of the sample. Sphericity was found to be 0.846, assuming zeolite 13X to be an octahedron crystal [12]. The particle diameter is ~ $3\mu m$.

Based on the porosity measurements, the crystal density of zeolite 13x was determined to be 1534.9 kg/m^3, which is within 4.5% of reported crystal density of zeolite 13X, 1470 kg/m^3 [10]. Once crystal density was confirmed, the porosity was estimated using Equation (1). It is important to note that Equation (2) may not be applicable to pressure-sensitive adsorbent crystals, as they tend to deform due to the applied load.

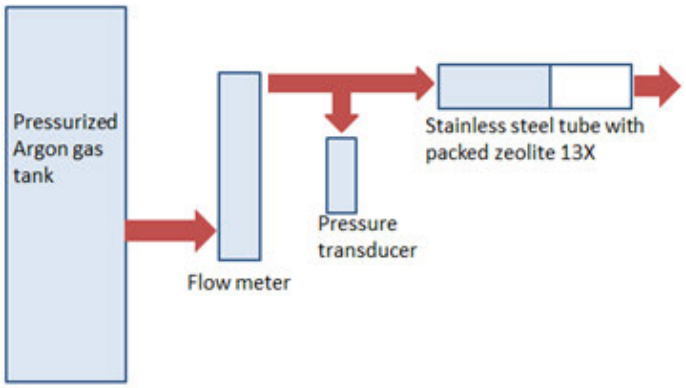

Figure 1. Schematic diagram illustrating the experimental set-up used for porosity measurement. The arrows indicate Argon flow direction

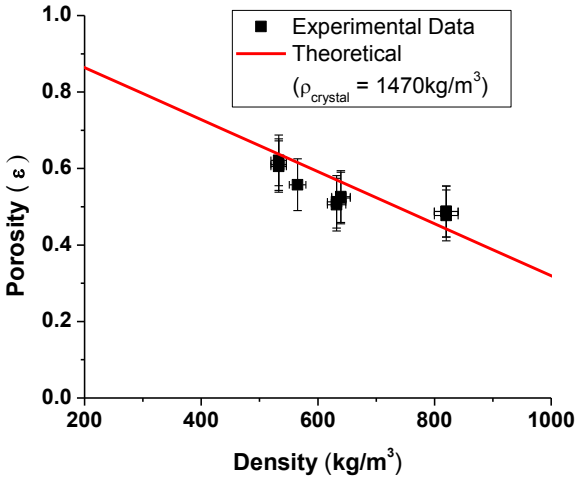

Figure 2. Density vs. Porosity of zeolite 13X

THERMOGRAVIMETRIC ANALYSIS

A vapor sorption analyzer (Q5000 SA, TA instruments) was used to characterize the adsorption isotherms of both the parent zeolite 13X and zeolite-binder composite. Aluminum hydroxide and zeolite composites were prepared from powdered zeolite 13X, and aqueous sodium aluminate and urea solutions (Sigma Aldrich). The sodium carbonated generated from the reaction was not removed as reported [9]. All samples were dried at 425 ^{o}C in air for 6 hours, and the isotherms were

subsequently measured at 40 °C, at 10% relative humidity, as shown in Figure 3. With aluminum hydroxide binder concentrations of 2.6, 6.4, 12.6, and 24.5 wt.%, at 10% relative humidity, the adsorption capacities were found to decrease by 4.9%, 10.6%, 31.2%, and 45.2%, respectively.

A TGA (DISCOVERY TGA, TA instruments) was used to characterize desorption characteristics. The overall cycling efficiency (or charging efficiency) of the ATB system depends on the rate and the input power for desorption. Powdered zeolite 13X samples bearing 30 wt.% water were heated to different temperatures ranging from 150 °C to 500 °C in the TGA. In order to observe and measure desorption characteristics in-situ, the temperature was ramped at 40 °C/min, with the relative humidity set at 0%. As evident in Figure 4, the threshold temperature required to dry zeolite 13X samples was found to be 250 °C and the time required for complete desorption was close to 10 minutes at 350 °C. However, it is to be noted that thermally-unstable adsorbents require further characterization since they degrade at higher temperatures.

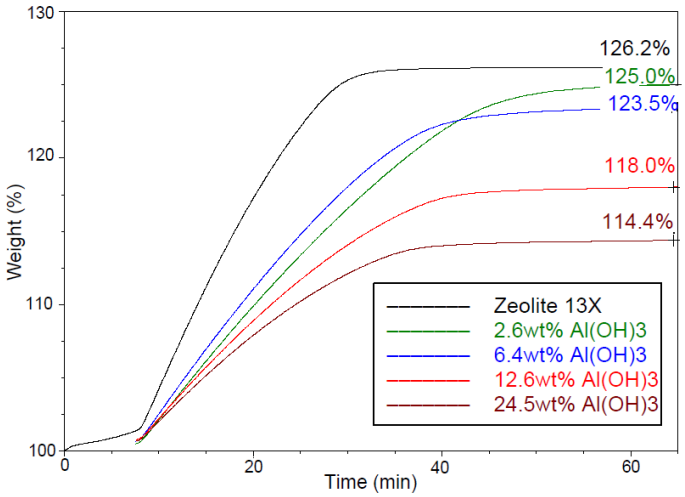

Figure 3. Adsorption capacity measured by sorption TGA at 40 °C with 10% relative humidity

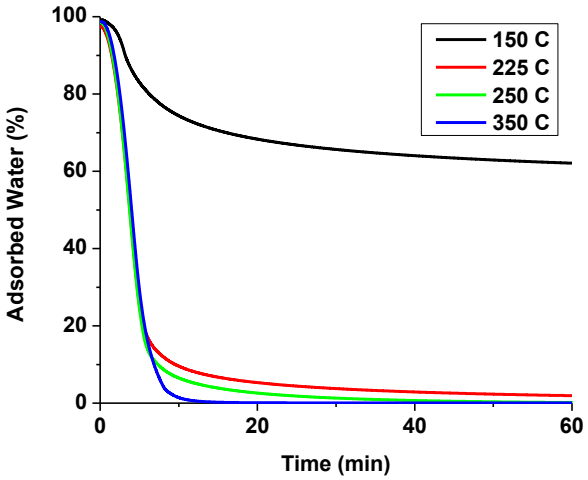

Figure 4. Desorption characteristics of Zeolite 13X (NaX) at various temperatures

BET ANALYSIS

BET surface area and adsorption analyses were performed on both the parent zeolite 13X and zeolite-binder composites to characterize the surface area and the micro-pore volume of each sample. The N_2 adsorption isotherms and the pore size distribution of each sample measured using the Quantachrome, Autosorb IQ2 Surface Sorption Analyzer are shown in Figure 5. The isotherms shown in Figure 5(a) clearly indicate a decrease in the N_2 uptake with the addition of the $Al(OH)_3$ binder. Furthermore, Table 1 shows the surface area and micro-pore volume measured by the BET analyzer. The surface area of the parent zeolite 13X was measured to be 649.2 m^2/g, corresponding to a pore volume 0.28 cm^3/g, while zeolite 13X with 24.5 wt.% aluminum hydroxide was measured at 393m^2/g, corresponding to a pore volume of 0.16 cm^3/g. These observations along with scanning electron microscopy (JEOL 6010LA SEM) (Figure 6) clearly indicate that the aluminum hydroxide binder blocks the micro-pores of zeolite 13X resulting in decreased adsorption capacity.

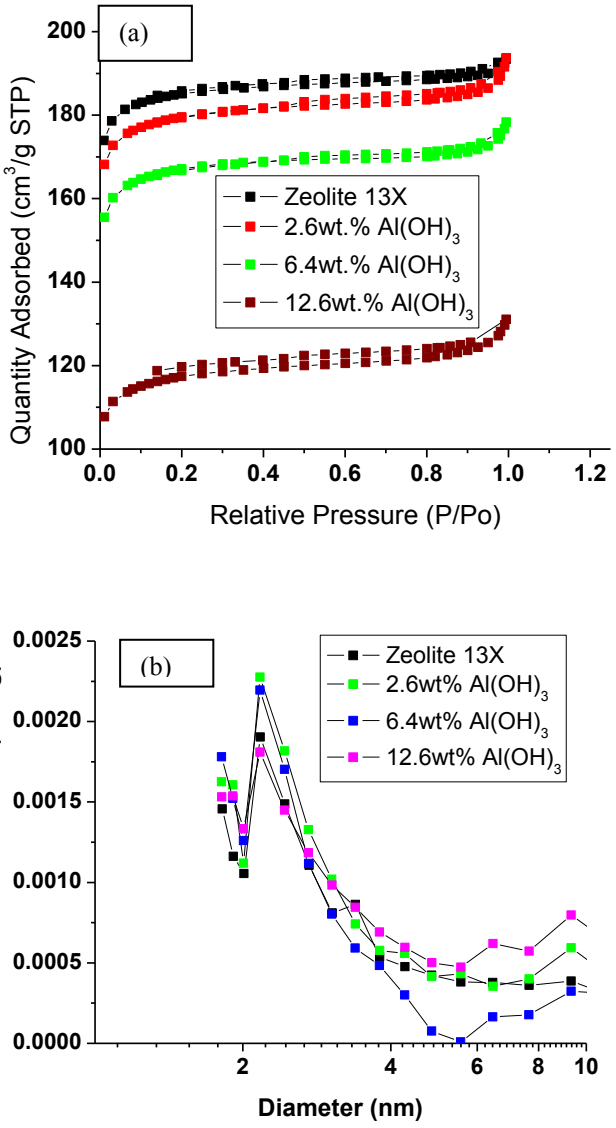

Figure 5. (a) Nitrogen adsorption isotherms and (b) pore size distribution of Zeolite 13X with and without $Al(OH)_3$ binder

Table. 1- Comparison of the BET surface area and the micro-pore volume of zeolite 13X with the addition of $Al(OH)_3$ binder

	BET Surface area (m^2/g)	Micro-pore Volume (cm^3/g)
Zeolite 13X	649.2	0.28
2.6wt% $Al(OH)_3$	617.25	0.28
6.4wt% $Al(OH)_3$	599.05	0.26
12.6wt% $Al(OH)_3$	557.94	0.24
24.5wt% $Al(OH)_3$	392.97	0.16

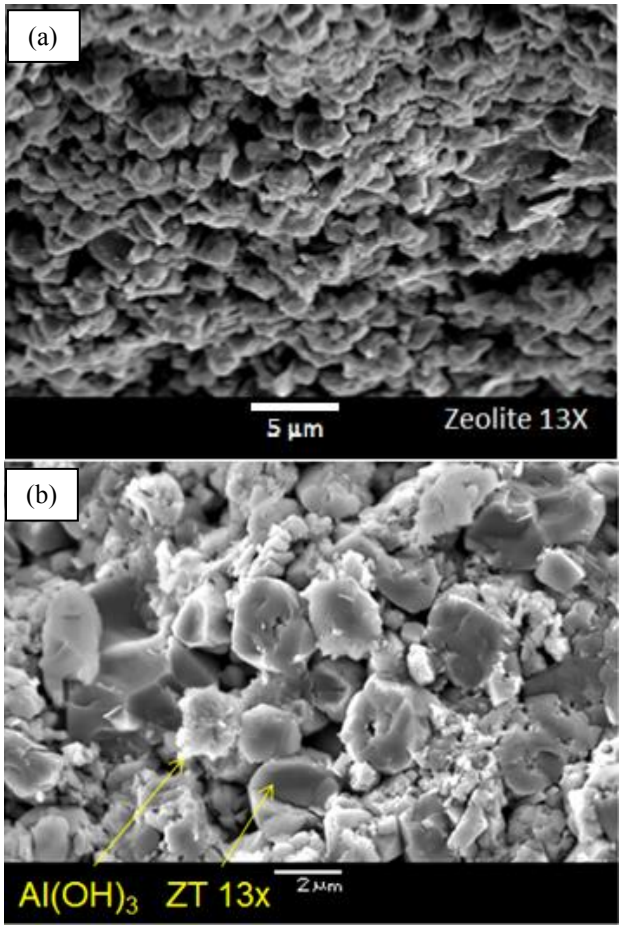

Figure 6. SEM images of (a) zeolite 13X and (b) zeolite 13X with 6.4wt.% $Al(OH)_3$

XRD ANALYSIS

Figure 7 shows X-ray diffraction (XRD) patterns of zeolite-binder composites after densification. As expected, distinctive XRD patterns of zeolite powder were found in the composite with 2.6 wt.% aluminum hydroxide, which confirms that there was no degradation in the crystal structure and the micro-pores of zeolite particles after densification. However, the intensity of the distinctive XRD patterns of the composite decreased as the amount of aluminum hydroxide increased in the composite. We attribute this to the amorphous structure of $Al(OH)_3$.

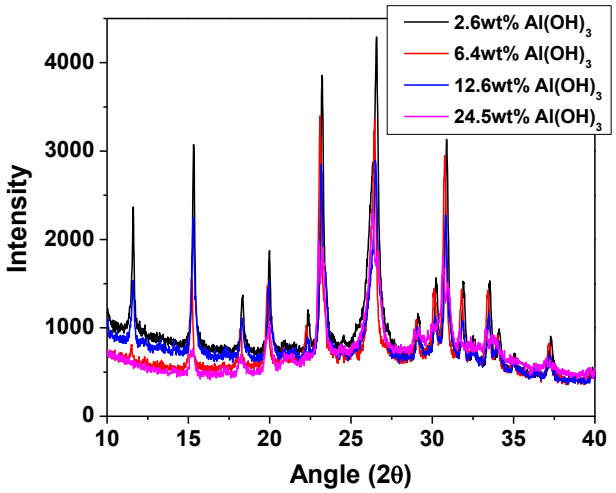

Figure 7. XRD patterns of Zeolite 13X with Aluminum Hydroxide binders

MEASUREMENT OF THERMAL CONDUCTIVITY

Typical adsorbents exhibit poor thermal conductivity, which is an undesirable characteristic for thermal energy storage. Both parent zeolite 13X and zeolite-binder composites were pressed into pellets of 12.7 mm diameter and 2 mm thickness. A graphite coating was applied to the surface prior to the thermal diffusivity measurements. The thickness of the graphite coating on the surface was found out to be negligible compared to the overall thickness of the sample, as shown by the SEM image in Figure 8. The thermal diffusivity of dehydrated and pressed samples were obtained using the Laser Flash Analyzer (Netzsch LFA 457 MicroFlash system) in an Argon environment, and the specific heat of each sample was measured using a differential scanning calorimeter (DSC, Mettler Toledo). The effective thermal conductivity, shown in Figure 9, is calculated using Equation (3):

$$k_{eff} = \rho \cdot \alpha \cdot c_p \quad (3)$$

where, ρ is the dehydrated density, α is thermal diffusivity, c_p is specific heat, and k_{eff} is effective thermal conductivity. The effective thermal conductivity increased from 0.23 W/mK to 0.415 W/mK with densification and the addition of 24.5 wt.% aluminum hydroxide as a binder. Thermal conductivity percolation was observed with the addition of 6.4 wt.% binder.

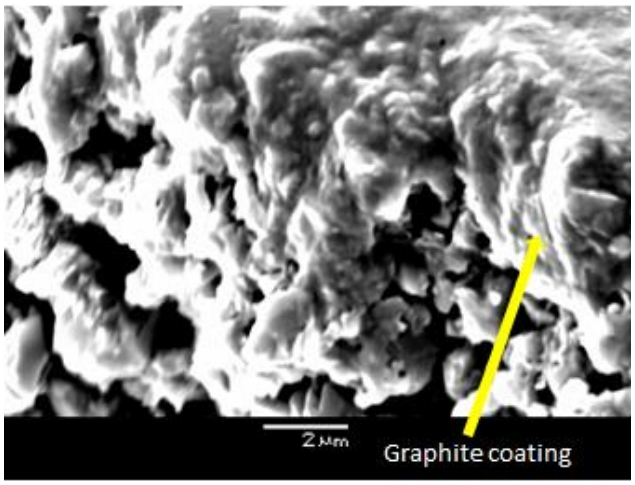

Figure 8. SEM image of interface between zeolite 13X and graphite coating

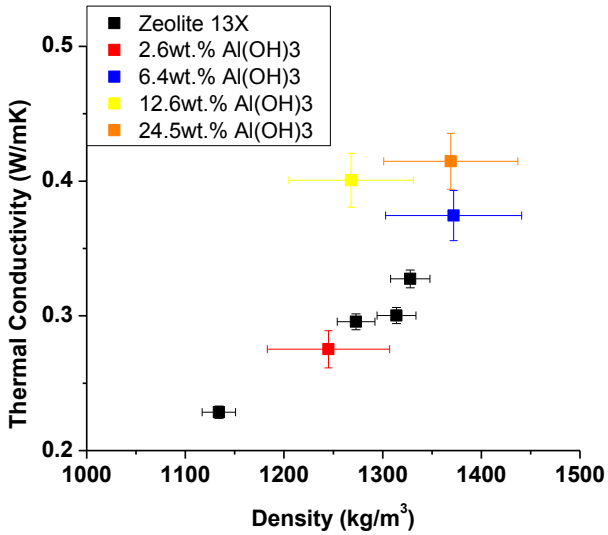

Figure 9. Effective thermal conductivity of Zeolite 13X and with binder at various temperatures

PREDICTION OF THERMAL CONDUCTIVITY

Heat transfer within the adsorption bed is a multi-phase problem. During ATB discharge, adsorbent is filled with water-vapor in both the gaseous and adsorbed phases. Predicting the thermal conductivity of adsorbent and binder composite with minimal number of experiments is necessary for optimizing the overall systems. However, a model that effectively predicts conductivity of adsorbent composite is not yet developed. Critical unknowns for the prediction of overall thermal conductivity include the zeolite crystal thermal conductivity, the thermal conductivity of the adsorbed phase, the percolation effect and threshold, as well as the interfacial resistance between crystals. In many cases, thermal conductivity of composite materials can be approximated with upper and lower bounds [13]. However, these bounds can be quite large, especially for granular materials. Various conductivity models have been proposed including series and parallel conductivity

models, Maxwell-Eucken models and the well-known effective medium theory. None of these models can make accurate predictions for two or more constituents. However, as demonstrated by Carson and co-workers [13], these predictive models can be used to estimate thermal conductivity bounds for composite materials. For example, zeolite composite can be modeled assuming the filling gas (in this case, Argon) as a continuous phase and zeolite particles as the embedded or the discontinuous phase. On the other hand, for comparison, the filling gas and zeolite can be considered as an embedded or discontinuous phase with the binder as a continuous phase.

In addition to setting the bounds on the overall thermal conductivity, the modified Zehner-Schlunder model [14], shown in equation (4) for packed spheres, effectively predicts the variation in the thermal conductivity as a function of the density, as shown in Figure 9.

$$\frac{k_{eq}}{k_g} = \left(1-\sqrt{1-\varepsilon}\right) + \frac{1-\sqrt{\varepsilon}}{\gamma} + \left(\sqrt{1-\varepsilon}+\sqrt{\varepsilon}-1\right)\cdot \left[\frac{b\cdot(1-\gamma)}{(1-\gamma\cdot b)^2}\ln\frac{1}{\gamma\cdot b} - \frac{b-1}{1-\gamma\cdot b}\right] \quad (4)$$

where $b = \left(\frac{1-\varepsilon}{\varepsilon}\right)^m$, $\gamma = \frac{k_g}{k_z}$, $m = 0.9676$, respectively.

In Equation (4), k_{eq} is effective thermal conductivity, k_g is thermal conductivity of filling gas, ε is outer-pore porosity, and k_z is the adsorbent thermal conductivity. However, modified Zehner-Schlunder model does not consider interfacial resistance between spheres; thus it overestimates the effective thermal conductivity of the composite material with an intrinsic conductivity of k_z. The predicted zeolite crystal conductivity can be as high as order of 1 W/mK [15]. As shown in Figure 10, the best match of the effective conductivity of zeolite composite was made when k_z was set as 0.385 W/mK for the density varying between 1000 and 1450 kg/m^3.

In order to theoretically estimate the thermal conductivity bounds for the zeolite-binder composite material, the thermal conductivity of aluminum hydroxide is required. This was measured with the same procedure outlined above using the laser flash analyzer. Thermal conductivity of the pelletized aluminum hydroxide was found to be 0.715 W/mK for a density of 2000 kg/m^3. It is to be noted that the thermal conductivity of the pellet may be quite different from intrinsic conductivity of aluminum hydroxide. Since the crystal density of aluminum hydroxide is known to be 2420 kg/m^3, the porosity of the pellet is estimated to be 17.4%. With a high packing density of aluminum hydroxide composite and a negligible contribution of the filling gas to the overall thermal conductivity, the model developed by Klemens [16] (Equation (5)) is used to estimate the effective thermal conductivity of 100% packed or a non-porous pellet of aluminum hydroxide . Equation (5) is valid for both isotropic and anisotropic particle shapes.

$$k_{binder} = \frac{k_{measured}}{1-\frac{4}{3}\varepsilon} \quad (5)$$

$k_{measured}$ is the experimentally measured effective thermal conductivity and ε is the porosity of the pelletized binder composite. k_{binder} denotes the conductivity of the binder composite with 100% packing fraction and was calculated to be 0.93W/mK. The conductivity of binder itself is relatively close to the conductivity of zeolite composite; therefore, percolation of aluminum hydroxide could play a significant role in enhancing the conductivity. Unlike zeolite crystals, aluminum hydroxide can indeed have a continuous 3-D phase, internal porosity material, thus making it a good candidate for both thermal and mechanical binders.

The conductivity of zeolite and binder composites was estimated using the modified Zehner-Schlunder and Klemens models, respectively. Using the proposed models, Maxwell Eucken (ME) and effective medium (EMT) theories as shown in equation (6) and (7); upper and lower bounds for zeolite-binder composite at density of 1370 kg/m^3 have been made as shown in Figure 11.

$$k_{ME} = k_1 \frac{2k_2+k_1-2(k_2-k_1)(1-v_2)}{2k_2+k_1+(k_2-k_1)(1-v_2)} \quad (6)$$

$$(1-v_2)\frac{k_1-k_{emt}}{k_1+2k_{emt}} + v_2\frac{k_2-k_{emt}}{k_2+2k_{emt}} = 0 \quad (7)$$

where v is volume fraction, k is thermal conductivity, 1 and 2 denote zeolite and binder composites, respectively. As shown in Figure 11, with a combination of existing models, thermal conductivity of composite material can be estimated accurately.

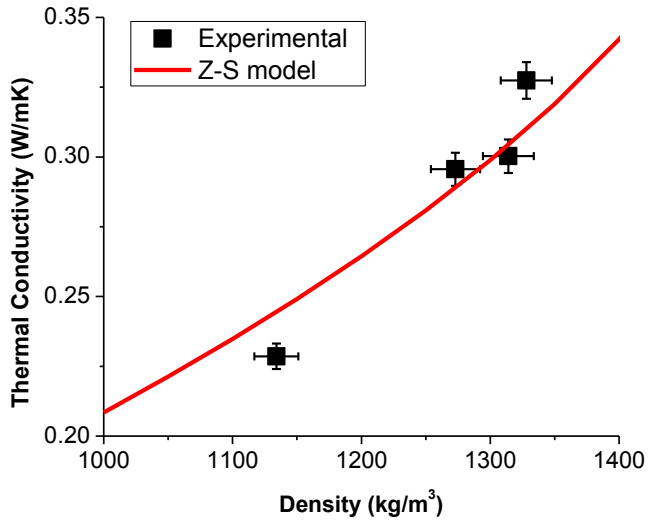

Figure 10. Effective thermal conductivity of Zeolite 13X and modified Zehner-Schlunder (Z-S) model

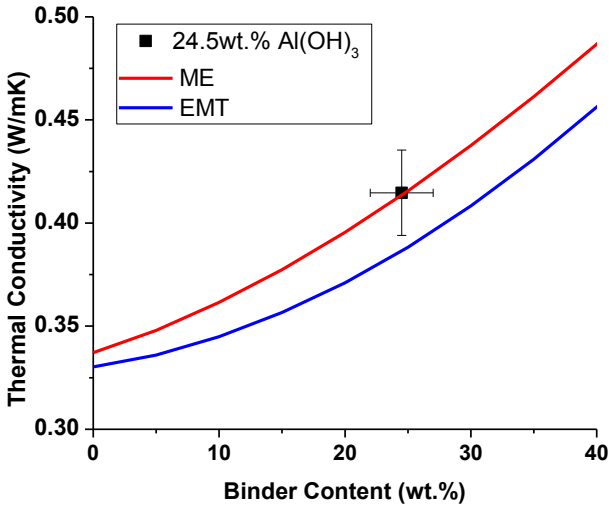

Figure 11. Upper and lower bound conductivities with experimental data at density of 1370kg/m^3

CONCLUSION

We report a detailed material characterization for the development of an advanced thermo-adsorptive battery to provide both heating and cooling for electric vehicles. Porosity, adsorption and desorption characteristics, BET micro-pore volume and surface area, and thermal conductivity were measured for pure zeolite 13X and its combination with aluminum hydroxide as a binder. Empirical models predicting the thermal conductivity of pure zeolite and its combination were also discussed and matched with experimental results. The addition of the aluminum hydroxide and densification resulted in a 81.4% increase in bulk thermal conductivity. However, aluminum hydroxide contributed to a significant decrease in the overall adsorption capacity, a 45.2% reduction at 10% relative humidity with the addition of 24.5 wt.% aluminum hydroxide as shown by sorption-TGA and BET analyses. The reduction in uptake was observed due to blockage of the micro-pores of zeolite crystal as evidenced by the decrease in the micro-pore volume.

Novel adsorbents, such as metal organic frameworks (MOFs) and synthetic zeolites can indeed be used for high-density thermal energy storage. However, their transport characteristics are not well characterized. The detailed experimental characterization and the theoretical framework presented in this paper for the prediction of thermal transport properties is essential for the development of advanced materials for their application in thermal energy storage.

ACKNOWLEDGMENTS

The authors gratefully acknowledge the support of Advanced Research Projects Agency-Energy (ARPA-E) with Dr. Ravi Prasher and Dr. James Klausner as program managers for providing financial support.

REFERENCES

1. Vijay, H., *Multi-Attribute Thermal Balancing on an Electric Vehicle, Focusing on Comfort and Fuel Economy.* SAE Technical Paper, 2012. **2012-01-2174**.
2. Restuccia, G., A. Freni, and G. Maggio, *A zeolite-coated bed for air conditioning adsorption systems: parametric study of heat and mass transfer by dynamic simulation.* Applied thermal engineering, 2002. **22**(6): p. 619-630.
3. Wang, D., Z. Xia, and J. Wu, *Design and performance prediction of a novel zeolite–water adsorption air conditioner.* Energy conversion and management, 2006. **47**(5): p. 590-610.
4. Eddaoudi, M., et al., *Systematic design of pore size and functionality in isoreticular MOFs and their application in methane storage.* Science, 2002. **295**(5554): p. 469-472.
5. Furukawa, H., et al., *Ultrahigh porosity in metal-organic frameworks.* Science, 2010. **329**(5990): p. 424-428.
6. Henninger, S.K., H.A. Habib, and C. Janiak, *MOFs as adsorbents for low temperature heating and cooling applications.* Journal of the American Chemical Society, 2009. **131**(8): p. 2776-2777.
7. Griesinger, A., K. Spindler, and E. Hahne, *Measurements and theoretical modelling of the effective thermal conductivity of zeolites.* International Journal of Heat and Mass Transfer, 1999. **42**(23): p. 4363-4374.
8. Liu, D., et al., *MOF-5 composites exhibiting improved thermal conductivity.* international journal of hydrogen energy, 2012. **37**(7): p. 6109-6117.
9. Pino, L., et al., *Composite materials based on zeolite 4A for adsorption heat pumps.* Adsorption, 1997. **3**(1): p. 33-40.
10. Sircar, S. and A.L. Myers, *Gas separation by zeolites.* Handbook of Zeolite Science and Technology, 2003: p. 1063-1105.
11. McCabe, W.L., J.C. Smith, and P. Harriott, *Unit operations of chemical engineering*. Vol. 3. 1956: McGraw-Hill Book Company New York.
12. Wadell, H., *Volume, shape, and roundness of quartz particles.* The Journal of Geology, 1935: p. 250-280.
13. Carson, J.K., et al., *Thermal conductivity bounds for isotropic, porous materials.* International Journal of Heat and Mass Transfer, 2005. **48**(11): p. 2150-2158.
14. Hsu, C., P. Cheng, and K. Wong, *Modified Zehner-Schlunder models for stagnant thermal conductivity of porous media.* International Journal of Heat and Mass Transfer, 1994. **37**(17): p. 2751-2759.
15. Coquil, T., et al., *Thermal conductivity of pure silica MEL and MFI zeolite thin films.* Journal of Applied Physics, 2010. **108**(4): p. 044902-044902-6.

16. Klemens, P.G., *Thermal conductivity of inhomogeneous media.* High Temp. High Press, 1991. **23**(3): p. 241-248.